The Institute of Space and Astronautical Science
Report SP No. 15, March 2003

Separation of 1699yr and 1866yr radiant points by use of the line detection method

By

Toshifumi YANAGISAWA,* Kouji OHNISHI,† Ken'ichi TORII,‡ Mitsuhiro KOHAMA,‡ Atsushi NAKAJIMA,* and David ASHER§

(1 February 2003)

Abstract: We have employed the new line detection method and successfully separated the two radiant points that correspond to the dust trails of Comet 55P/Tempel-Tuttle's perihelion passages in 1699 and 1866. This method integrates pixel values of a CCD image along a line direction, which enables us to detect 30 times fainter meteors than usual detection methods. It can also determine the angle of the line direction precisely. Radiant points of 2001 Leonids derived by this method were found to be consistent with those predicted by McNaught and Asher.

1. INTRODUCTION

Leonid meteor storms were observed at various places in Japan on 2001 November 18th UT. Dust generated over the past few centuries by Comet 55P/Tempel-Tuttle caused this phenomenon. The dust trail theories that predict when and where the meteor storm will occur are well studied recently by various groups (Kondrat'eva, et al. (2000), Asher, and McNaught (2001), Lyytinen, et al. (2001), McNaught, and Asher (2001)). These theories can predict more accurately than the classical theory by using gravitational perturbation and solar radiation pressure. They are now widely accepted by the successful predictions of meteor activities in the last few years.

McNaught, and Asher (2001)

predicted 2000 meteors of Leonid in ZHR at 17:24 UT and 8000 at 18:13 UT will fall around East Asia. They also predicted the coordinates of radiant points belonging to the 1866 return of the comet (4 revolutions ago, hereafter we call 4-rev) and the 1699 return (9 revolutions ago, hereafter we call 9-rev) precisely. The separation between the two radiant points is 0.14 degree on the sky. If these radiant points are separated observationally, that becomes powerful support to the dust trail theory.

* National Aerospace Laboratory of Japan, 7-44-1 Jindaiji-higashi-machi, Chofu, Tokyo 182-8522, Japan.
† Nagano National College of Technology, 716 Ohaza-tokuma, Nagano, Nagano 381-8550, Japan.
‡ Riken, 2-1 Hirosawa, Wakoh, Saitama 351-0198, Japan.
§ Armagh Observatory, College Hill, Armagh, BT61 9DG, United Kingdom.

This document is provided by JAXA.

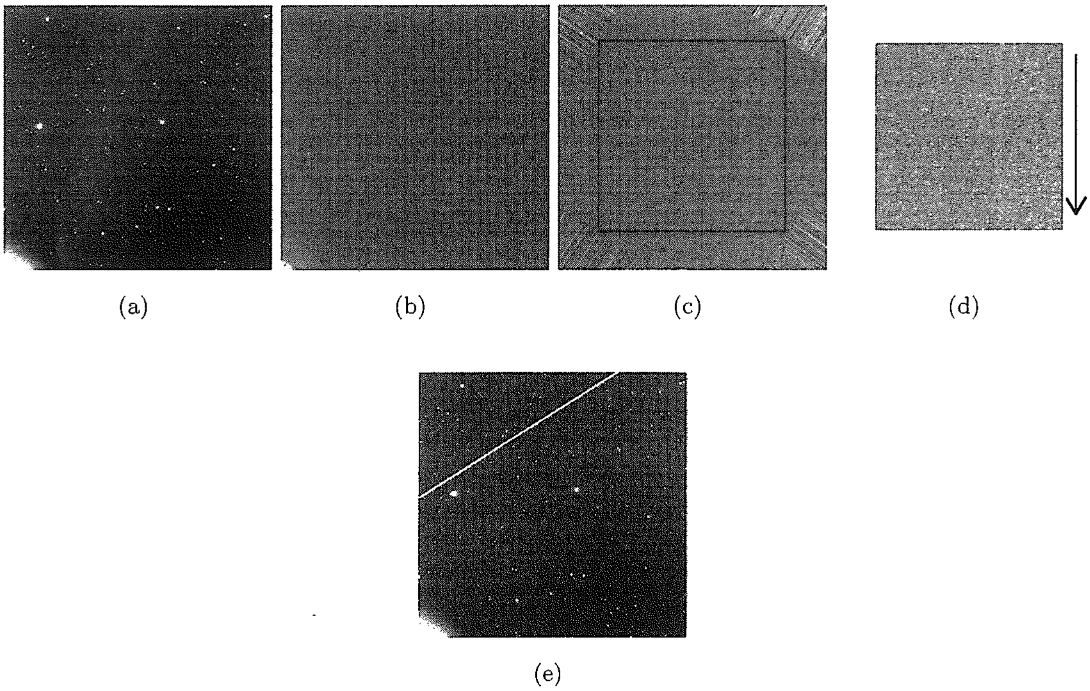

Fig. 1: The process of the line detection method.

We tried to separate the two radiant points using a new technique called the line detection method. This method integrates pixel values of a CCD image along a line direction, which enables us to detect 30 times fainter meteors than usual detection methods. In order to determine radiant points of meteors, a stereo observation for the triangulation analysis is ordinarily carried out. However, we observed Leonid meteor storms from a single site and used the line detection method to determine each radiant point precisely. A large number of meteors of Leonid enable us to carry out such a challenging observation.

2. THE LINE DETECTION METHOD

Meteors, low earth orbit(LEO) satellites and LEO debris leave streaks on a CCD image when they pass through the field of view of the CCD camera. When they are dark, the streaks are not recognized on CCD images. However, their signals that are buried in the sky background noise must remain. We developed an image processing technique, the line detection method, to extract effects of the streaks created by meteors, LEO satellites and LEO debris. In this method, median values of all pixels of every line along one direction are calculated that reduces the sky background noise efficiently as Equation (1).

$$\sigma_{median} = \frac{1.2}{\sqrt{N}}\sigma_{individual} \tag{1}$$

Here N is the number of pixels along one direction. The factor 1.2 is calculated from Monte Carlo simulations(Pennycook G., (1998)). Calculating an average can reduce the sky background noise more effectively than calculating a median. However, an average is influenced by

This document is provided by JAXA.

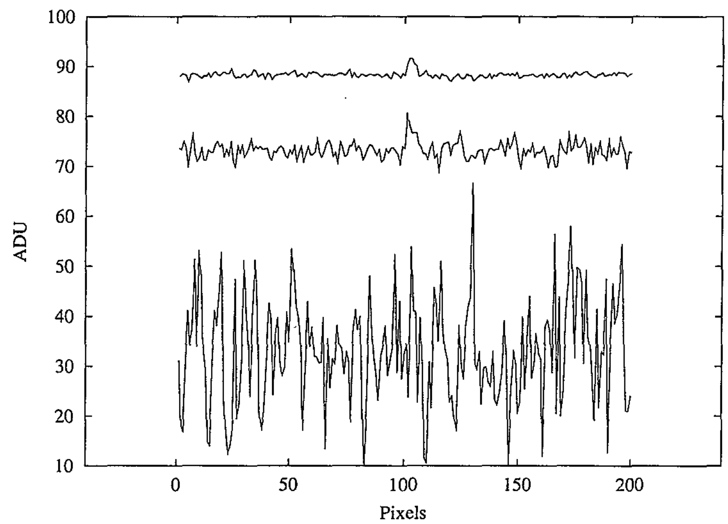

Fig. 2: A sample result of the line detection method.

extremely high signals such as fixed stars, cosmic rays and thermal noises. Fig.1 shows the process of the line detection method. Fig.1(a) is a raw CCD image. The white spots are fixed stars. In this image, no lines are observable at a first sight. Fixed stars are first removed by masking or subtracting a sequent image (Fig.1(b)). Then the image is rotated at a proper angle and the effective region with no influence from the rotation process is cut out (Fig.1 (c)). Finally median values of all pixels of every line along the arrow are calculated (Fig.1(d)). The last two parts of the process (Fig.1(c) and Fig.1(d)) are repeated for every angle of interest to detect weak invisible lines.

Fig.2 shows an example of a line effect detected in an image by using the line detection method. The horizontal and vertical axes show pixel numbers perpendicular to the direction and the values of each pixel respectively. Constant values are added to the upper two lines for clear presentaion. The bottom line shows the noise level of a raw CCD image. The middle one shows the median values of every 20 pixels along the direction. The line effect is visible at the center. The top one shows the median values of all pixels along the direction. The effect is clearly comfirmed. From the rotation angle and the coordinate of the effect, the actual position of the detected line is determined as shown in Fig.1(e).

The pixel number along one direction of recent CCD cameras is about a few thousands. Equation (1) indicates the line detection method can detect 30 to 40 times darker meteors and LEO objects than usual methods. We calculated the ability of the line detection method in some cases. When a $50mm$ camera lens and a 2K×2K back-illuminated CCD camera are used for the observation of meteors, they are expected to detect meteors of 8.5 magnitude and determine their directions precisely. When the one-meter telescope and the back-illuminated CCD camera of the Bisei Spaceguard Center are used for the observation of LEO debris, they are expected to detect $3cm$ LEO debris at $200km$, $6cm$ debris at $400km$ and $10cm$ debris at $1000km$ using the line detection method. The Bisei Spaceguard Center is founded by the Japan Space Forum in Okayama Prefecture, Japan, and used solely for the observation of space debris and NEOs (near earth objects)(Isobe, and Japanese Spaceguard Association (1999)).

This document is provided by JAXA.

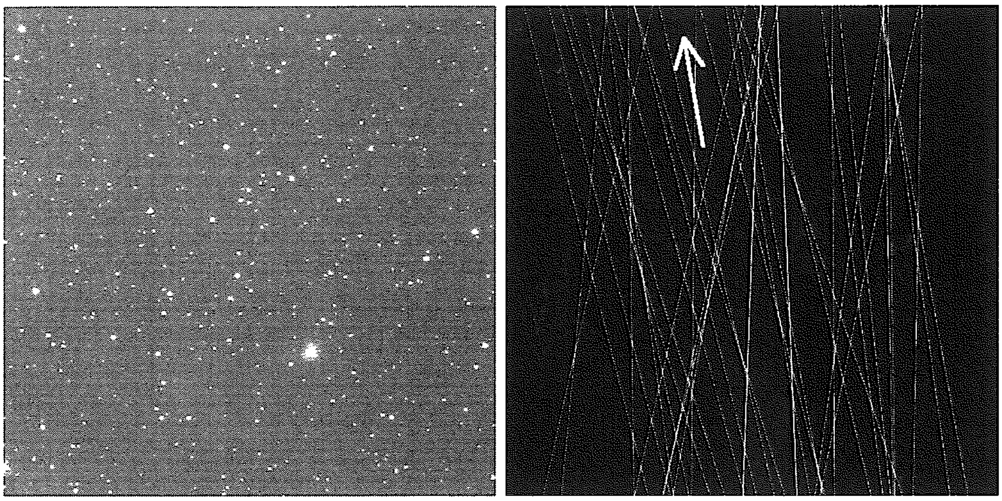

(a) (b)

Fig. 3: A raw CCD frame of region-1 with a 10-second expousre time((a)) and detected lines in 50 frames of region-1 taken at from 18:20:35(UT) to 18:32:08(UT)((b)). The arrow in (b) shows the direction to the radiant points.

3. OBSERVATION

The observation was carried out on November 19, 2001, at the Akeno observatory of the Institute of Cosmic Ray Research, the University of Tokyo. The site is at $138°30'E, 35°47'N, 900m$ altitude. We observed two regions near the radiant points predicted by McNaught, and Asher (2001). In order to determine the radiant points precisely, the two regions are set to make a right angle with the radiant points. The coordinates of each region are listed in Table 1.

Table 1: Detail of the observed regions

No. of region	R.A.	Dec	angle	pixel size($''/pixel$)
1	$10h17m11s$	$28°22'33''$	$4.44°$	5.02
2	$09h50m25s$	$20°48'43''$	$207.87°$	9.26

A "FCC-104B" 1K×1K back-illuminated CCD camera manufactured by Nakanishi Image Laboratory Co. Ltd. and an "AP7" 512×512 back-illuminated CCD camera manufactured by Apogee were used for the observation of region-1 and 2 respectively. Each camera was mounted on a Takahashi's "ϵ-160" 16cm hyperbolid astrograph refractor. Focal length of the telescope was $530mm$ and the cameras cover a $1.4° \times 1.4°$ and a $1.3° \times 1.3°$ respectively. These telescopes were mounted on equatorial mounts. The CCD cameras were cooled using a thermo electric cooler. Each camera took numerous images of each region continuously with a 10-second exposure time for the "FCC-104B" and a 20-second exposure time for the "AP7". 173 frames were taken for region-1 between 17:56:20 UT and 18:41:59 UT and 100 frames for

This document is provided by JAXA.

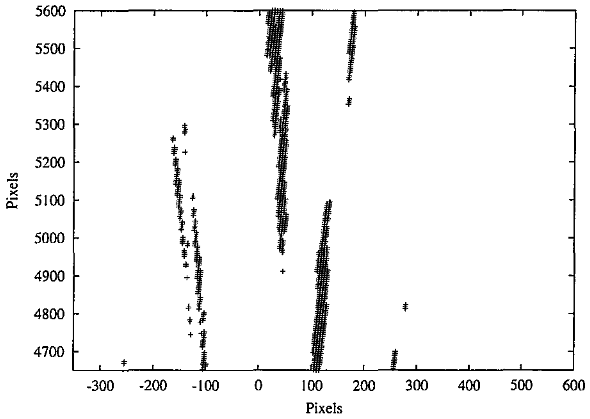

(a)

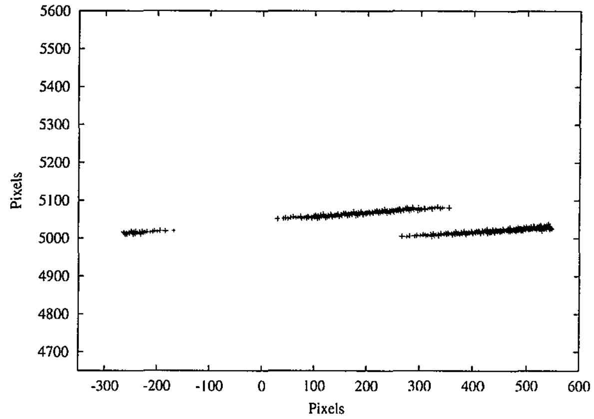

(b)

Fig. 4: Results of the line detection method. (a) and (b) show results from the data of region-1 and 2 respectively.

region-2 between 17:56:23 UT and 18:44:33 UT. Maximum time of rev-9's radiant point at Tokyo predicted by McNaught, and Asher (2001) was 17:24 UT and that of rev-4's was 18:13 UT.

4. ANALYSIS AND RESULTS

First, all the frames were dark frame subtracted and flat-fielded. The two observed regions were shifted slowly at every frame because of poor alignments of the pole axes of the equatorial mounts. Therefore a central pixel of the first frame of each region was assumed to be the origin and the shift value of every frame to the origin was investigated using some fixed stars on the frame. The coordinates, the angle to the declination line and the pixel size of each first frame were calculated by comparing fixed stars on the frame and the Guide Star Catalog. The results are shown in Table 1. The line detection method described in Section 2 was carried out to all the frames. At this analysis, fixed stars were removed by subtracting a sequent image. All the frames were rotated ± 20 degrees from the direction of the predicted radiant points with 0.1 degree step and lines more than a 4.4-sigma significant were recorded. From the rotation angle and the coordinate where the effect of the line was detected, the inclination and the constant of the detected line were calculated. The inclinations and the constants of the detected lines for each frame are converted to those for the first frame using the shift value mentioned above. As a result of analyzing all the frames, we detected 279 lines on region-1 and 75 lines on region-2. A raw CCD frame and detected lines in 50 frames are shown in Fig.3. The arrow in Fig.3(b) shows the direction to the radiant points.

All the lines were extrapolated to the region around the predicted radiant points using the inclinations, the constants and the angles to the declination line listed in Table 1. The density of the lines was then investigated. The number of lines within a radius of 75 arc seconds was counted and the coordinates that have many lines in the circle were recorded. Fig.4(a) and 4(b) show the results from the data of region-1 and 2 respectively. X and Y-axis show pixel values

This document is provided by JAXA.

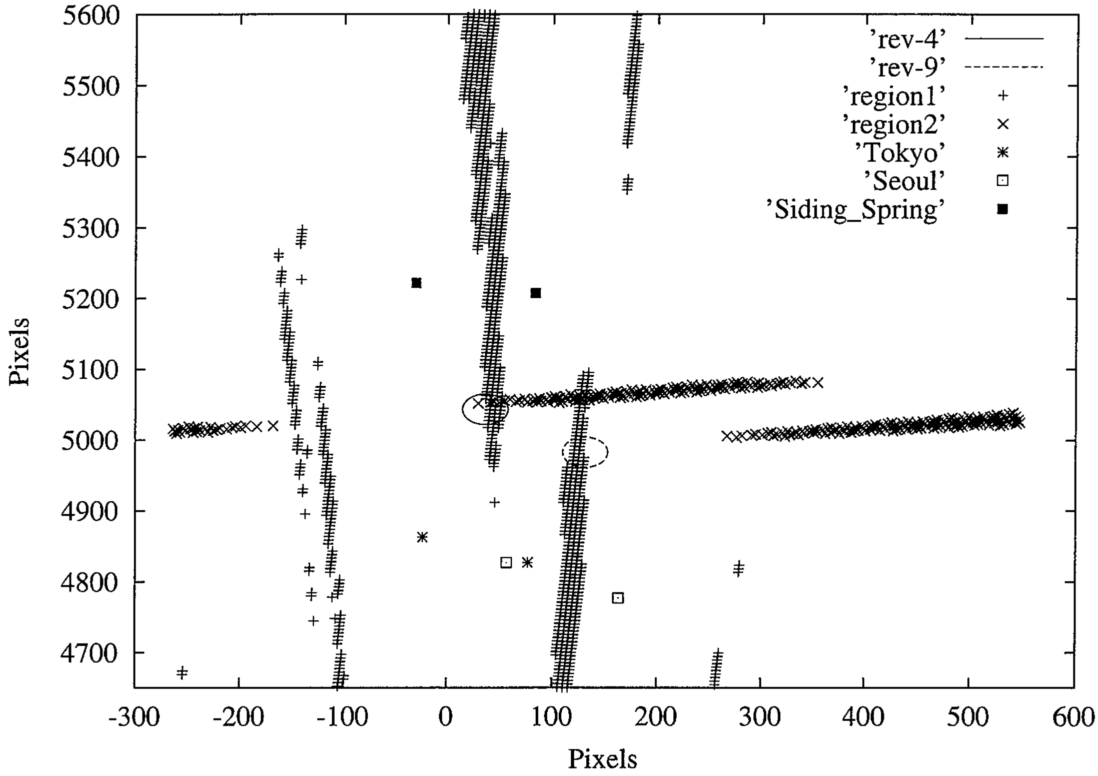

Fig. 5: A combined result of region-1 and 2 accompanied with the predicted radiant points of rev-4 and 9 for some cities. Solid and dashed lines show the radiant points of rev-4 and 9 obtained from this observation respectively.

from the origin of region-1. 1 pixel corresponds to about 5 arc seconds in the sky. R.A value increases when X value decreases and Dec value increases when Y value decreases. The points containing more than six lines in the circle are plotted in Fig.4(a). There are two dense regions around (40,5200) and (120,4900) in Fig.4(a). Similarly, the points of more than three lines were plotted in Fig.4(b). There are also two dense regions around (200,5050) and (450,5000) in Fig.4(b). The central position of region-2 is (4486.5,5319.5).

5. DISCUSSION

Fig.5 shows the combined result of region-1 and 2 accompanied with the predicted radiant points of rev-4 and rev-9 for some cities. It is hard to conclude that two radiant points were separated only from the result of region-2 because each dense region of Fig.4(b) consists of a small numbers(three) of lines. However, two dense regions of Fig.4(a) consist of 12 and 8 lines respectively. It is obvious that two radiant points (rev-4 and rev-9) are separated each other. Assuming that the result of region-2 is true, we can calculate two radiant points from the results of region-1 and 2. From the arrangement of the dense regions of Fig.4(a), Fig.4(b) and the predicted radiant points for some cities, it is better to consider the upper-left dense regions of both the figures are due to the radiant point of rev-4 and the other pair of the lower-right dense regions come from that of rev-9. The latter pair does not have a cross point in Fig.5. However, there is a large error bar along the line of sight from region-2. We used a 360×360 pixel region

This document is provided by JAXA.

of the 512×512 CCD camera to determine directions of region-2's lines. Every detected line has a ±0.16° error on its direction. The points determined from these lines in Fig.4(b), have at least a ±200 pixels error along the line of sight from region-2. This error helps to make a cross point of the latter pair. Four lines for every dense region from the centers of the corresponding regions are calculated using the method of least square. The coordinates of the radiant points of rev-4 and rev-9 are as follows.

R.A.=154.245° ± 0.037, Dec=21.349° ± 0.024 (2000) for rev-4
R.A.=154.112° ± 0.018, Dec=21.433° ± 0.034 (2000) for rev-9

The errors contain the standard deviations of the line directions and errors that the line directions contain individually as mentioned above. We did not consider the zenith attraction and the diurnal aberration to extract these coordinates. The separation between the two radiant points is 0.157° ± 0.059 that agrees well with that of McNaught, and Asher (2001). The solid and dashed lines in Fig.5 show the radiant points of rev-4 and 9 determined by this observation respectively. We proved that the dust trail theory is correct from these results.

ACKNOWLEDGMENTS

We thank Prof. Masahiro Teshima (the University of Tokyo) and all of the staff of the Akeno Observatory for their kind support of our observations.

REFERENCES

Kondrat'eva E.D., Murav'eva I.N., Reznikov E.A., 2000, Solar System Research 34, 237
Asher D.J., McNaught R.H., 2001, WGN 28, 134
Lyyrinen E., Nissinen M., Van Flandern T., 2001, WGN 29, 110
McNaught R.H., Asher D.J., 2001, WGN 29, 156
Pennycook G., 1998, MS thesis, Univ.Auckland
Isobe, S., Japanese Spaceguard Association., 1999, Adv. Space Res. 23, 33

This document is provided by JAXA.